2018 University Turbine Systems Research Project Review Meeting
October 30 – November 1, 2018

Turbine: Gas Turbine Thermal Analysis

Tom I-P. Shih
School of Aeronautics and Astronautics, Purdue University

Mark Bryden
Ames National Laboratory, U.S. Dept. of Energy

Robin Ames and Rich Dennis
National Energy Technology Laboratory, U.S. Dept. of Energy

For **gas turbines**, efficiency increases with **“turbine inlet T and P”**

Today, **aircraft:** 2,000 °C for aircraft

power gen: 1,500 °C for H-Class (40+% efficiency)

1,600 °C for J-Class (45%% efficiency in combined cycle)

Goal: 1,700 °C w/ CMC & ½ cooling flow

BUT, Ni-based superalloy (+TBC) up to **2400 °F (1,300 °C)**

THUS, **cooling is needed** for all parts of GT in contact with the hot gases via internal and/or film cooling

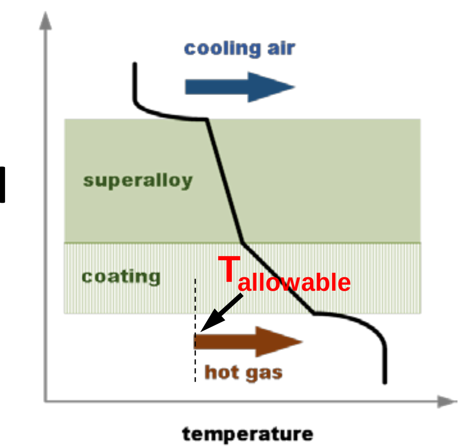

Since 15 to 30% of the air that enter the compressor is used to cool the turbine, **want better materials (e.g., CMC) and better cooling technology** so that cooling flow can be reduced.

Goal? Increase GT efficiency by **halfing the cooling flow**.

How? Further improve understanding of the fundamentals. Details matter since we want to **operate near the maximum allowable material T and ∇T**

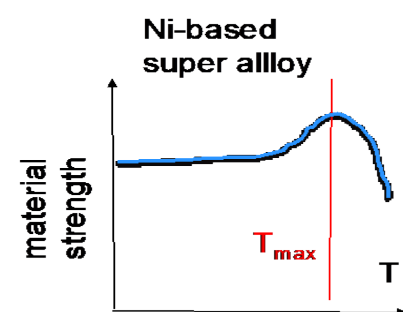

Focus: **pin-fin arrays**

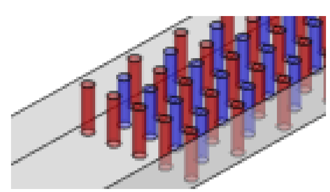

Some recent highlights:

- **LES of film cooling**: *GT2018-76170 (also, J. of Turbomachinery, 2018); AIAA 2018-4734*
- **LES of internal cooling**: *GT2018-75530 (also, J. of Eng. for Gas Turbine & Power, 2018; GT2018-75535, AIAA 2018-4432*
- **Reduced-order model for rim-seal:** *GT2018-75802*

Provided

- Insights on when RANS fails (e.g., unsteady separations that URANS can't predict)
- Turbulent statistics such as **u'v', u'T', u'P', … to guide RANS model development**
- Guidelines on how to do LES and hybrid RANS-LES right for internal and film cooling (e.g., -5/3, Celik Criteria, concurrent simulation for LES inflow BC of internal flows, RANS-LES interface BCs).

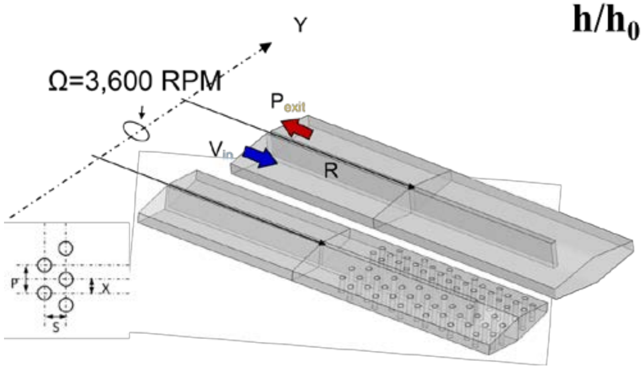

GT2018-75530

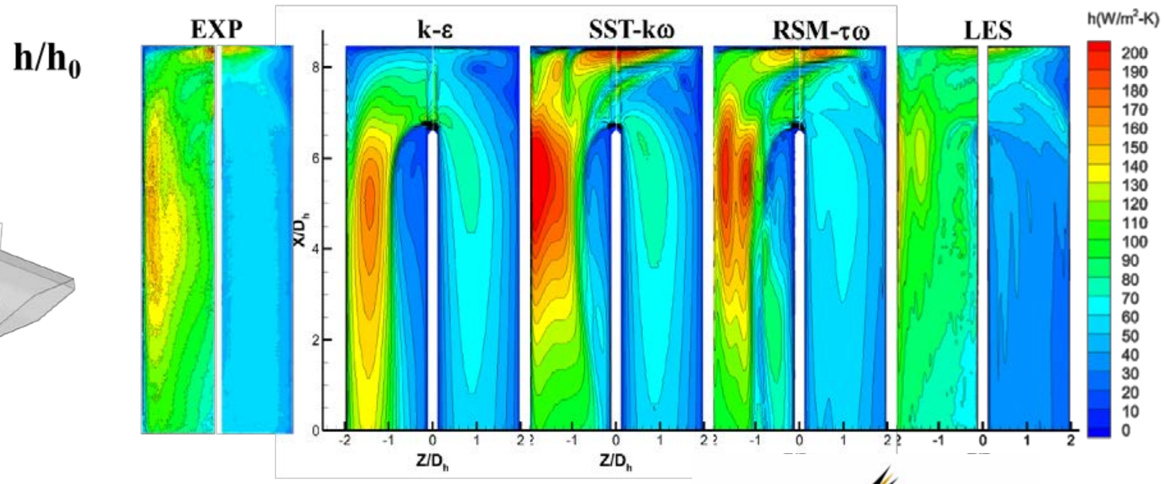

U.S. DEPARTMENT OF ENERGY · NATIONAL ENERGY TECHNOLOGY LABORATORY · AMES LABORATORY Creating Materials & Energy Solutions U.S. DEPARTMENT OF ENERGY · PURDUE AERONAUTICS & ASTRONAUTICS

Current efforts:

Just got 1 year access to 6,000 cores with 4TB RAM for a year + unlimited number of licenses of PowerFlow from EXA + … to do grid and time-resolved LES, where **all data (e.g., all statistics) will be made public**:

Under lab and engine operating conditions!

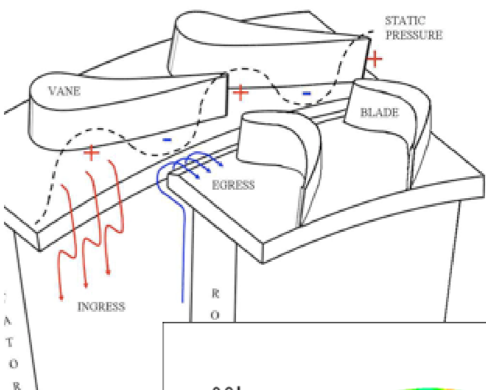

RIM SEALS:
Bath Configuration: 1.0 stage 360 degrees

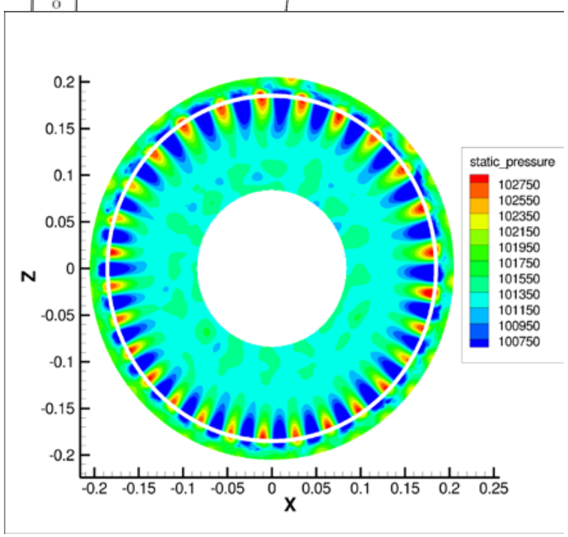

BLADE TIP in 1.5 stage:
Flat, squealer, … w/ and w/o film cooling

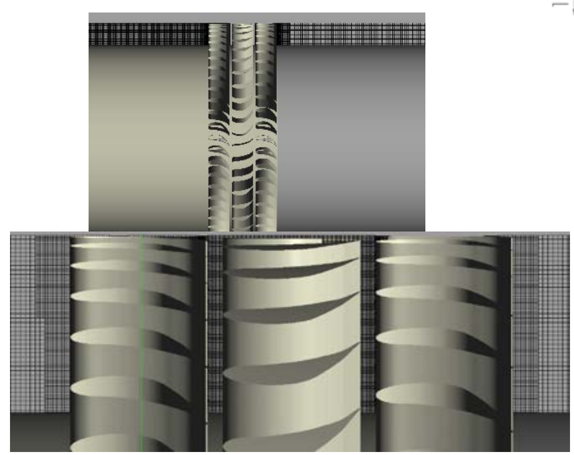

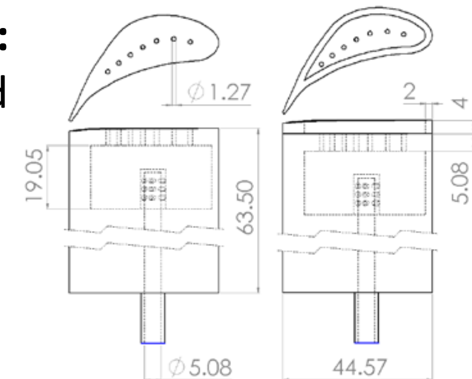

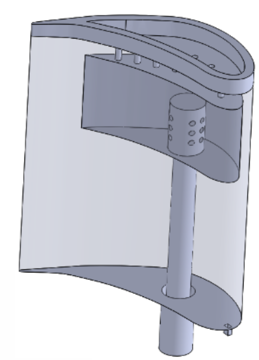

Effects of High Heating Loads on the Unsteady Flow and Heat Transfer in a Cooling Passage with a Staggered Array of Pin Fins

Chien-Shing Lee and Tom I-P. Shih
School of Aeronautics and Astronautics, Purdue University

- Introduction
- Objective
- Problem Description
- Formulation/Numerical Method
- Results
- Summary

Previous Work on Pin-Fin Arrays

Flow and heat transfer in channels with pin-fin arrays have been studied extensively by **experiments and computations:**

Heat exchanger (bank of tubes)

See reviews by Kakac et al. (2012), Incropera & DeWitt (2002) and work by **(Exp.)** Zukauskas (1972), Kays & London (1955), … **(CFD/Model)** Khan (2006), Benhamadouche & Laurence (2003), Wilson & Bassiouny (2000), Watterson (1999), Launder & Massey (1978), ...

GT airfoil trailing edge (short pin-fin arrays)

- **Reviews:** Ekkad, Chyu & Cunha (2014), Han et al.(2013), Armstrong and Winstanley (1988), …
- **Exp. Averaged:** Ekkad (2012), Lawson (2011), Siw (2012), Chyu (1998, 1999, 2010), Van Fossen (1982, 1984), Simoneau (1984), Metzger (1982), …
- **Exp. Time-Resolved:** Ostanek and Thole (2012), Ames, et al (2005, 2006, 2007)
- **CFD RANS:** Shih, et al (2017), Li, Jiang & Ligrani (2016), Siw & Chyu (2012), Chi & Shih (2011), …
- **CFD URANS & LES w/ RANS wall treatment:** Delibra (2009, 2010), ….

Review: short pin-fin arrays of internal cooling

Most experimental (**Metzger, Simoneau, Van Fossen, Chyu, Siw, Ames, Lawson, Ostanek, Thole, Ekkad, …**) and computational (**Delibra, Chi, Shih, Chyu, Li, Jiang, Ligrani, …**) studies of internal cooling passages with pin fins have focused on time-averaged flow and heat transfer quantities.

Parameters studied: HTC and DP = f(Re, pin-fin height & shape, spacings between fins, number of rows).

Ames and Dvorak (2006), Ames et al. (2005, 2007), Ostanek & Thole (2012) measured the unsteady flow and heat transfer induced by the shedding of the wakes behind the pin fins = f(fin geometry & spacing).

Delibra et al. (2008, 2009), Paniagua et al. (2014) reported URANS and LES studies to assess the capabilities of turbulence models for predicting the unsteady flow and heat transfer in a short pin-fin array.

Shih, Lee, & Bryden (2017) reported RANS on effects of heat load.

Objective

Since

- GTs operate at high heating loads with considerable temperature variation along cooling ducts, and
- Flow & HT about pin fins are unsteady and only steady RANS has been used to study high heating loads

the objectives of this study are

- understand the effects of high heating loads on the nature of unsteady flow and HT by using RANS, URANS, and hybrid LES
- Assess capability of RANS, URANS, and hybrid LES to predict heat-transfer coefficient.

in an internal cooling passage with a staggered array of pin fins.

Problem Description

staggered array of short pin-fins

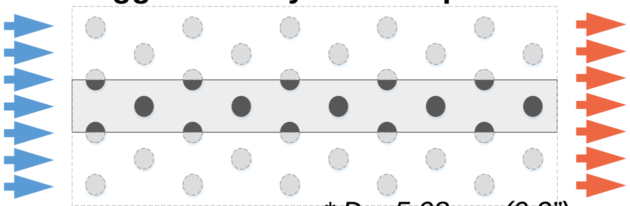

* D = 5.08mm (0.2")

Pin-fin height: $H/D = 1$ (short pin)

Test zone width: $L/D = 25$

Streamwise pin spacing: $S_x/D = 2.5$

spanwise pin spacing: $S_y/D = 2.5$

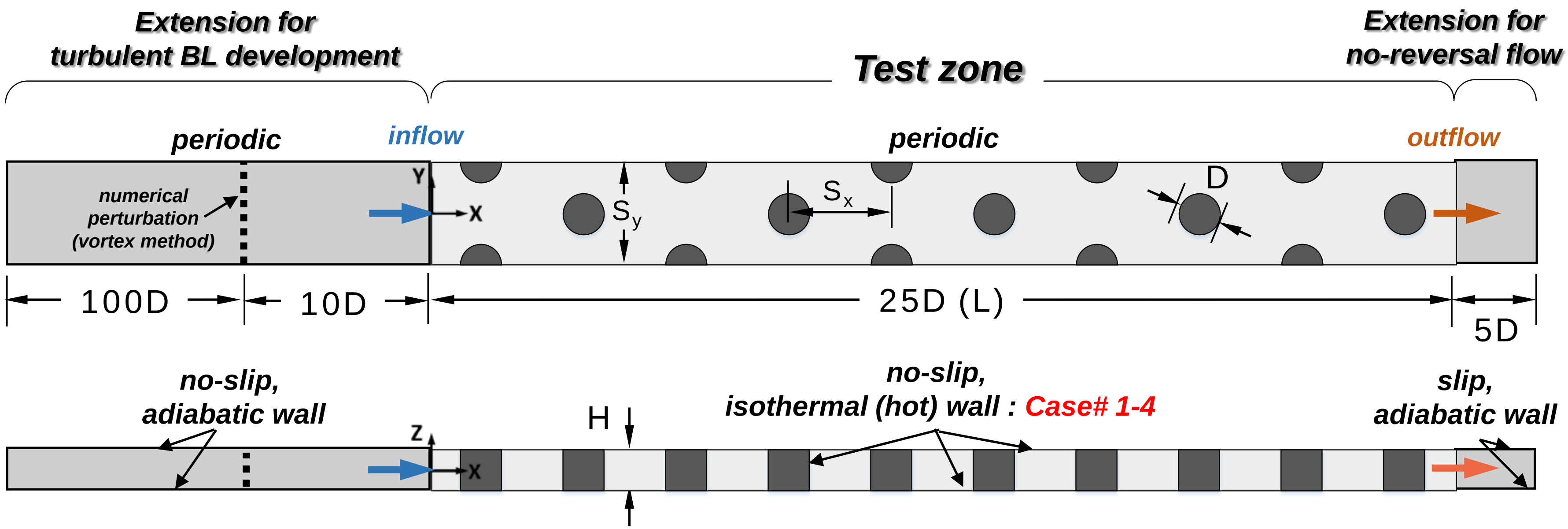

Cooling gas (air)

$\dot{\mathbf{m}} = 0.00636\ \mathrm{kg/s}$

$\mathbf{T_c} = 673\ \mathrm{K}$

$\mathbf{Re_{D,\,x/D=1.25}} = \dfrac{\rho V_{max} D}{\mu(T_b)} = 25{,}000$

$\mathbf{P_b} = 25\ \mathrm{bars}$

Case#	T_w (heat load)	T_w/T_c
1	678 K	1.01
2	873 K	1.30
3	1,073 K	1.60
4	1,273 K	1.90

Formulation / Numerical Method of Solution

Formulation:

- **Gas:** compressible, thermally perfect gas with k(T), C_p(T), and μ(T)
- **Turbulence:**
  - RANS & URANS based on SST
  - hybrid - URANS in near-wall region and LES away from wall via SAS model to transition between URANS and LES (Menter et al. 2010)

Code: ANSYS-Fluent v17.1

Algorithm:

- 2^{nd}-order accurate in time
- PISO with 2^{nd}-order upwind for the advection terms & central for diffusion terms

Convergence Criteria for Unsteady Solutions:

iterate until converged at each time step (typically 20 to 30 iterations per time step) - normalized residual at the end of each time step for continuity< 10^{-5}, momentum< 10^{-5}, and energy<10^{-7}, turbulence quantities < 10^{-5}.

PS: We are working on exploring and developing hybrid methods with distinct boundaries between RANS and LES. Results TBA.

U.S. DEPARTMENT OF ENERGY NETL NATIONAL ENERGY TECHNOLOGY LABORATORY AMES LABORATORY PURDUE AERONAUTICS & ASTRONAUTICS

Grid System

Grid	Mesh #1	Mesh #2*	Mesh #3
Hex cell (million)	4.9	10.1	11.2
Cell spacing (max.): $\Delta X^+/\Delta Y^+/\Delta Z^+$	91/91/43	45/45/21	22/22/10
Wall y^+ : endwall/pin	0.79/1.33	0.67/0.99	0.61/0.87

*** Mesh #2 was used in this study**

Monitor: center line of the flow field

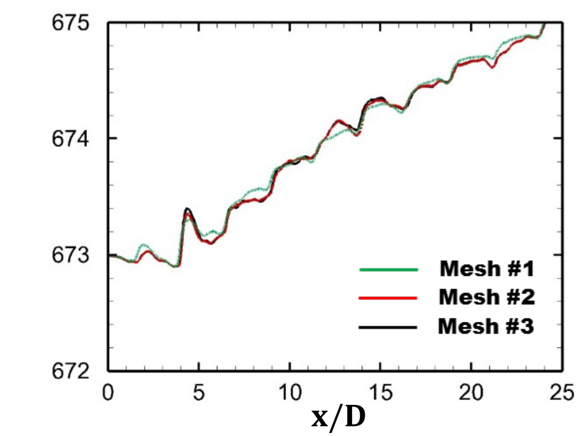

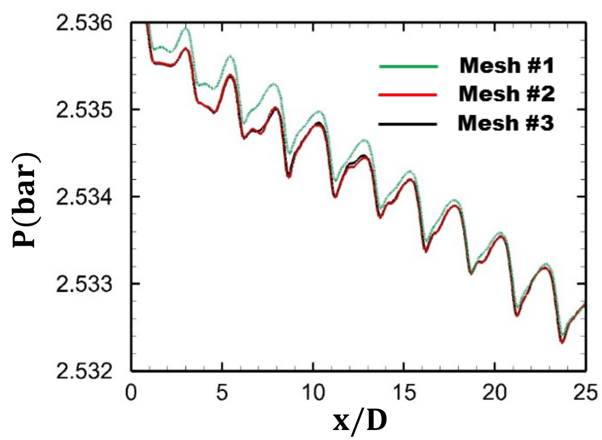

Monitor: center line on the bottom wall

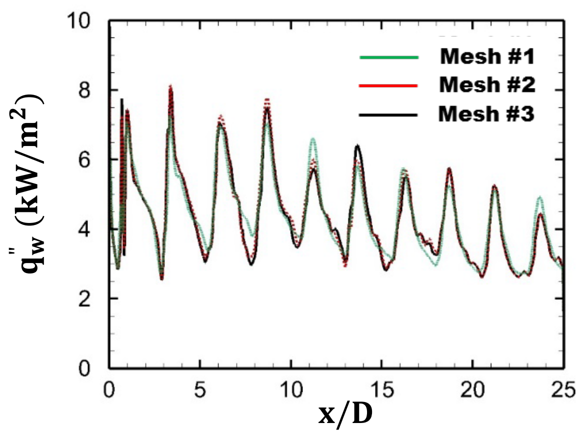

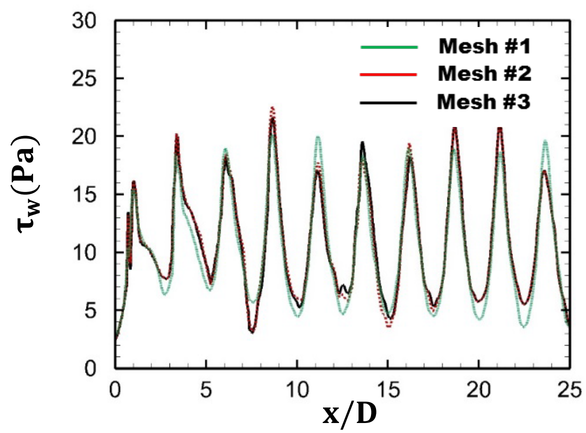

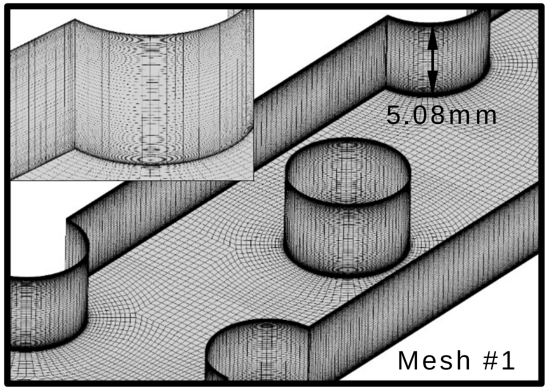

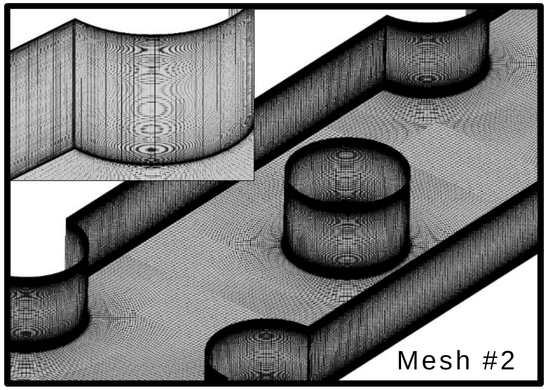

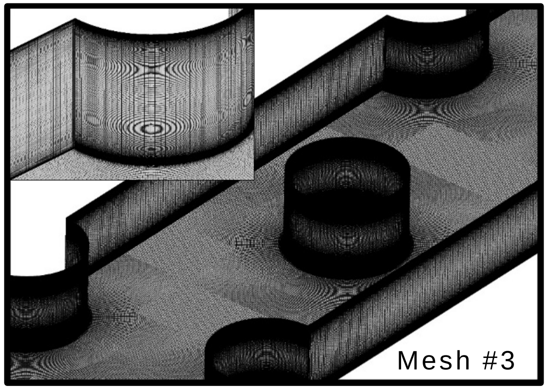

Validation: Mean Surface Nusselt Number

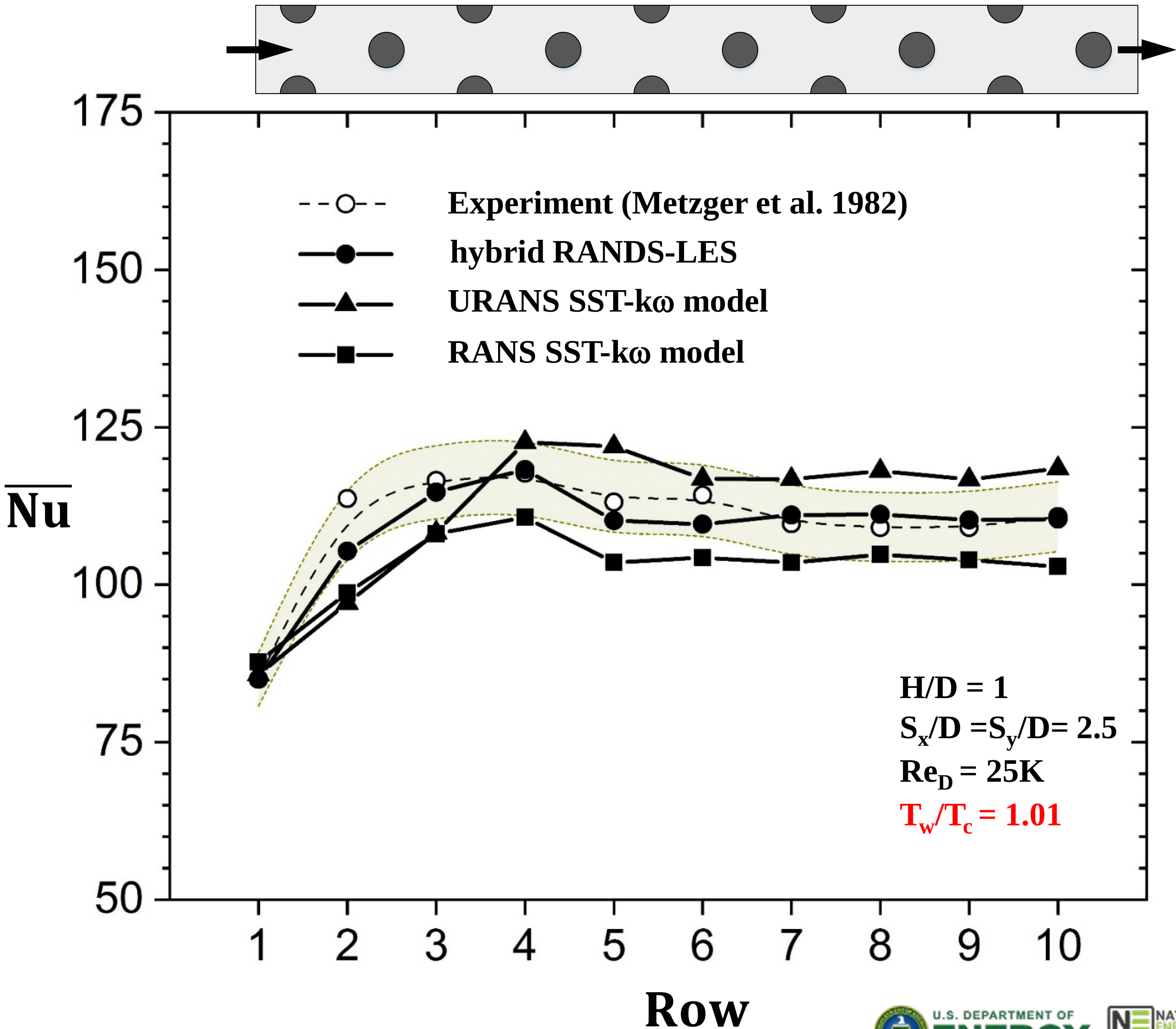

$$\overline{Nu} = \frac{\bar{h}D}{k(T_b)}$$

Good agreement with experimental data for Re=25K was achieved for the zonal-averaged wall Nu.

Validation: Mean Surface Nusselt Number

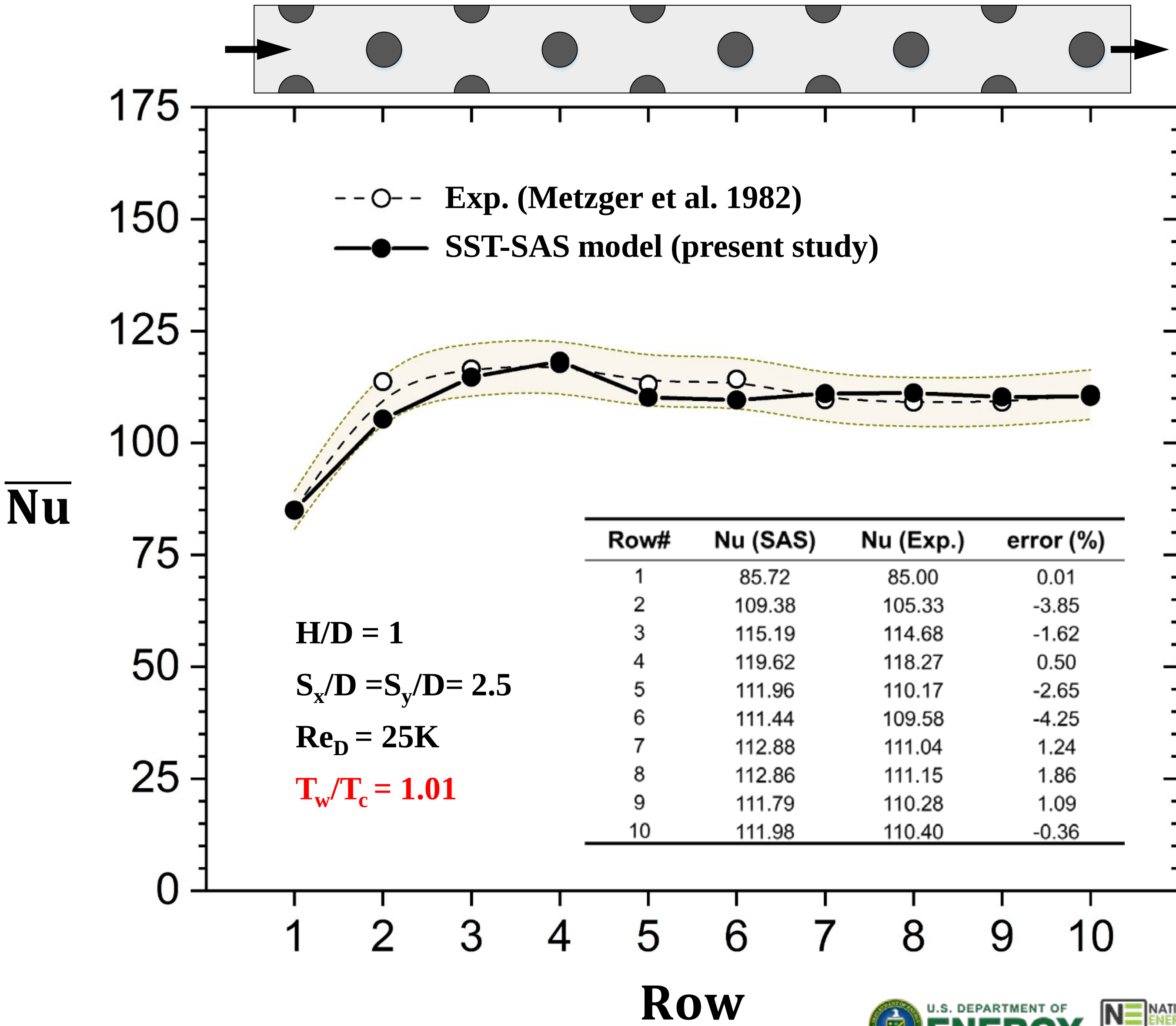

Row#	Nu (SAS)	Nu (Exp.)	error (%)
1	85.72	85.00	0.01
2	109.38	105.33	-3.85
3	115.19	114.68	-1.62
4	119.62	118.27	0.50
5	111.96	110.17	-2.65
6	111.44	109.58	-4.25
7	112.88	111.04	1.24
8	112.86	111.15	1.86
9	111.79	110.28	1.09
10	111.98	110.40	-0.36

$$\overline{Nu} = \frac{\bar{h}D}{\overline{k(T_b)}}$$

Good agreement with experimental data for Re=25K was achieved for the zonal-averaged wall Nu.

Mean Flow: T_b, Re, Pr, Nu

Bulk Temperature through the Duct

Regionally-averaged $\bar{T}_b$ along the passage as a function of heat loads (T_w/T_c)

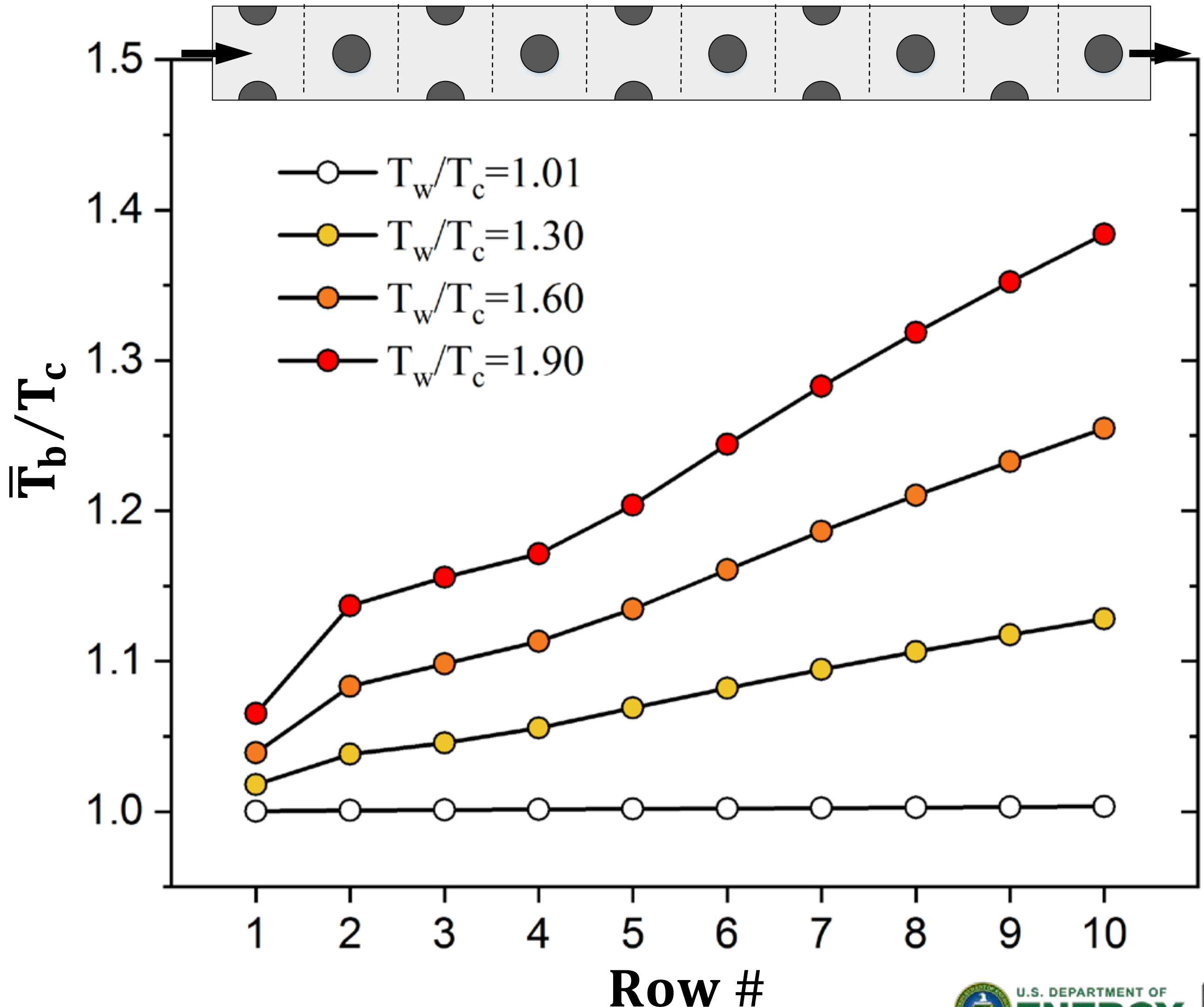

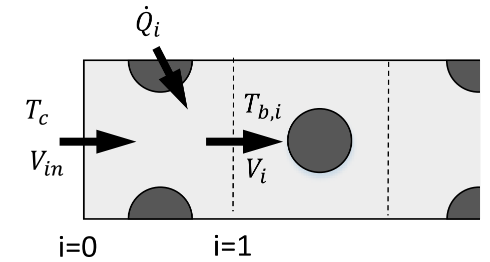

$$T_{b,i} \equiv \frac{C_{p,c}}{C_{p,i}} T_c - \frac{1}{2C_{p,i}}\left(\bar{V}_i^2 - V_{in}^2\right) + \frac{\sum \dot{Q}_i}{\dot{m} C_{p,i}}$$

- T_b increases over the rows as the flow is being heated by the hot wall.
- T_b can arise 22% from the inlet to the outlet.

U.S. DEPARTMENT OF ENERGY · NATIONAL ENERGY TECHNOLOGY LABORATORY · AMES LABORATORY · PURDUE AERONAUTICS & ASTRONAUTICS

Reynolds Number through the Duct

Regionally-averaged $\overline{Re}_D$ along the passage as a function of heat loads (T_w/T_c)

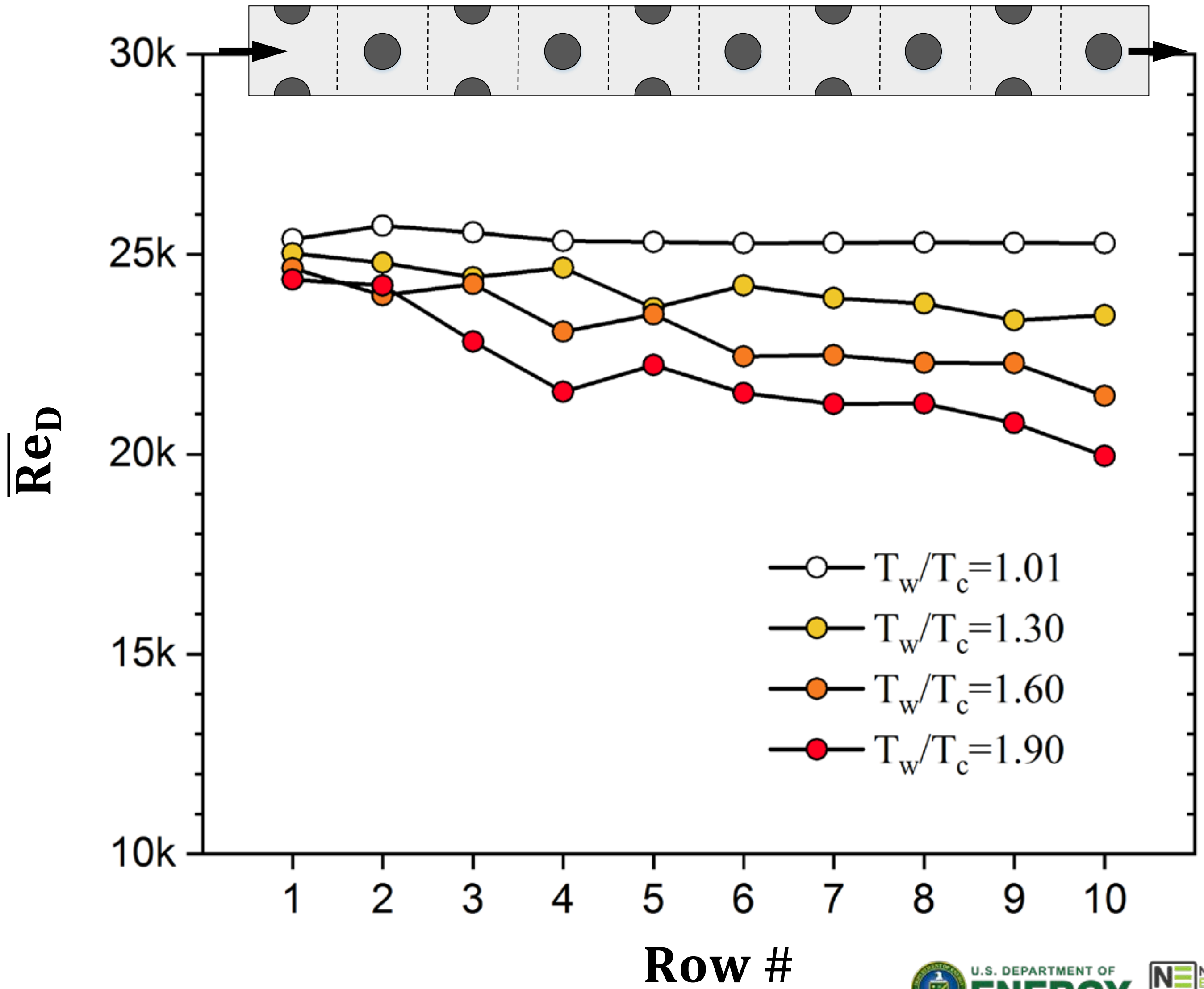

$$\overline{Re}_D = \frac{\bar{\rho}\bar{V}_{max}D}{\overline{\mu(T_b)}}$$

- Re_D decreases over the rows because $\mu(T_b)$ increases.
- Re_D can decrease by up to 20% from the inlet to the outlet when T_w/T_c = 1.9.

U.S. DEPARTMENT OF ENERGY
NATIONAL ENERGY TECHNOLOGY LABORATORY
AMES LABORATORY
PURDUE AERONAUTICS & ASTRONAUTICS

Prandtl Number through the Duct

Regionally-averaged $\overline{Pr}$ along the passage as a function of heat loads (T_w/T_c)

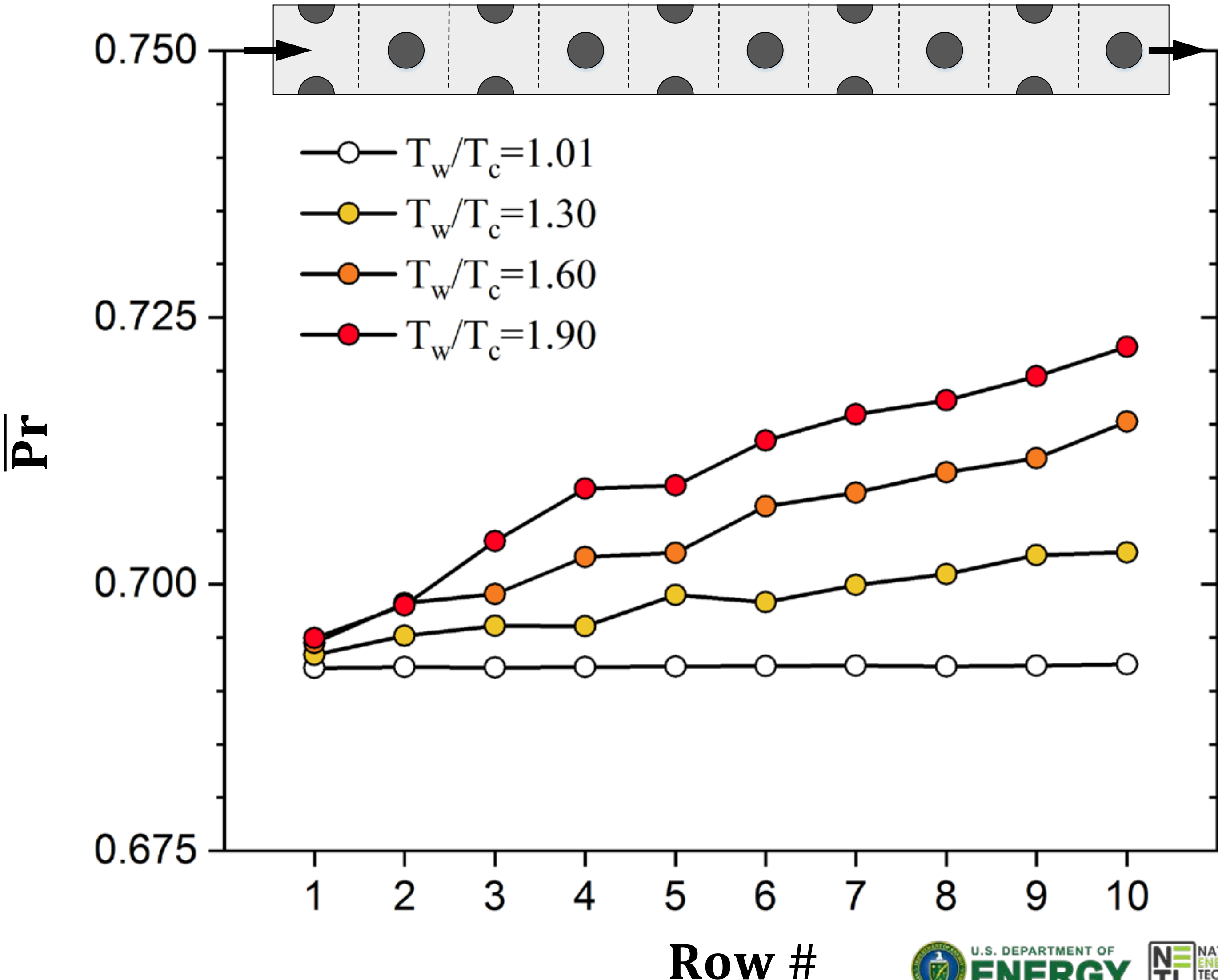

$$\overline{Pr} = \frac{\overline{\mu(T_b)}\,\overline{C_p(T_b)}}{\overline{k(T_b)}}$$

- Pr increases over the rows since the flow transport properties (μ, C_p, k) change locally with the increasing bulk temperature.
- Pr can increase 4% from the inlet to the outlet.

Nusselt Number through the Duct

Regionally-averaged $\overline{Nu}$ along the passage as a function of heat loads (T_w/T_c)

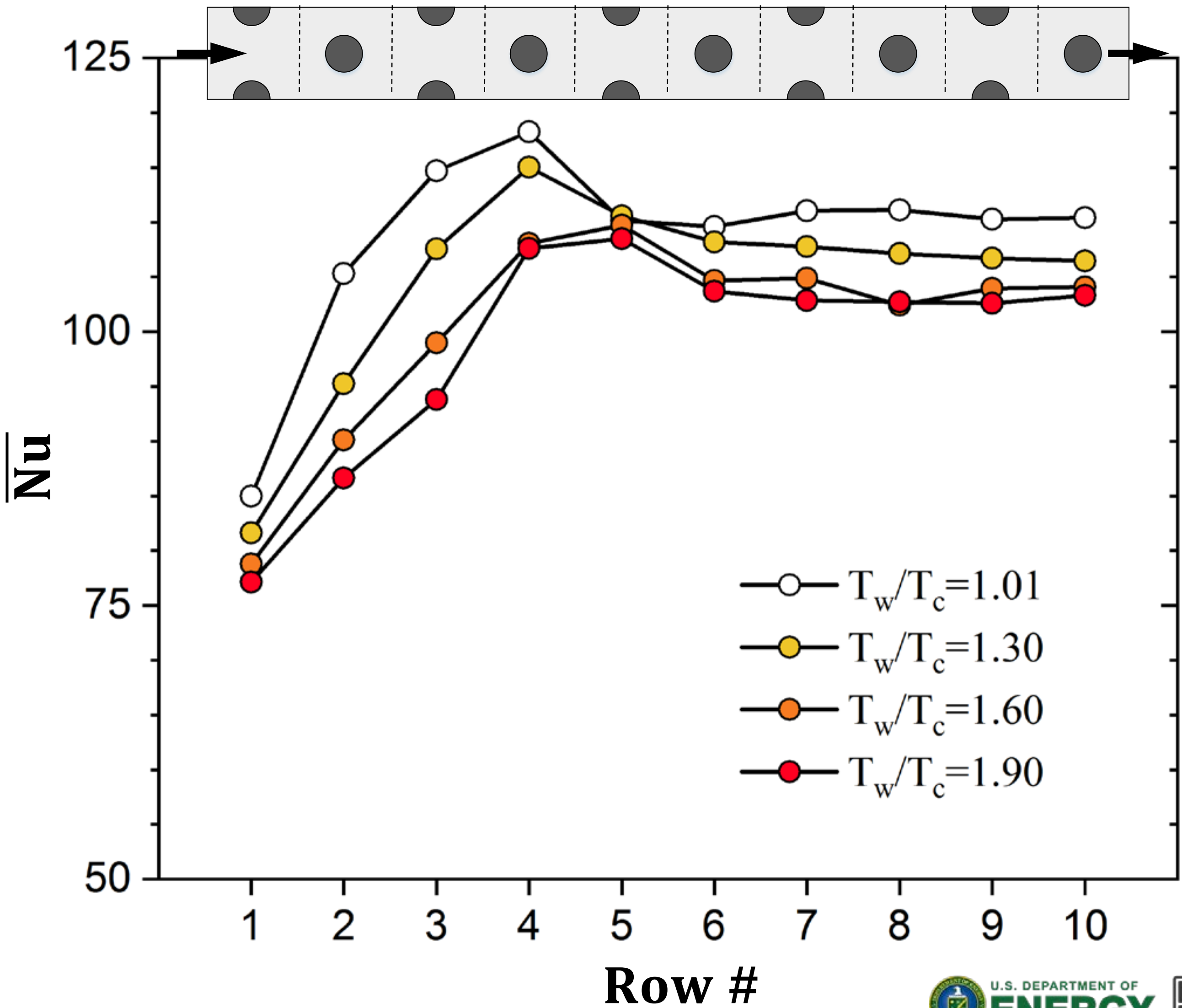

$$\overline{Nu} = \frac{\bar{h}D}{\overline{k(T_b)}}$$

- As the heating load increases, the mean Nu number decreases.
- Nu increases over the front rows in the entrance region and reaches to its maximum at the 4th row.
- Nu is not strongly affected by the heating loads at the 5th row, where there is a transition from the entrance region (Rows 1-4) to the fully developed region (Rows 6-10).

Boundary-Layer Separation

Flow Separation Line on 1st Pin Fin

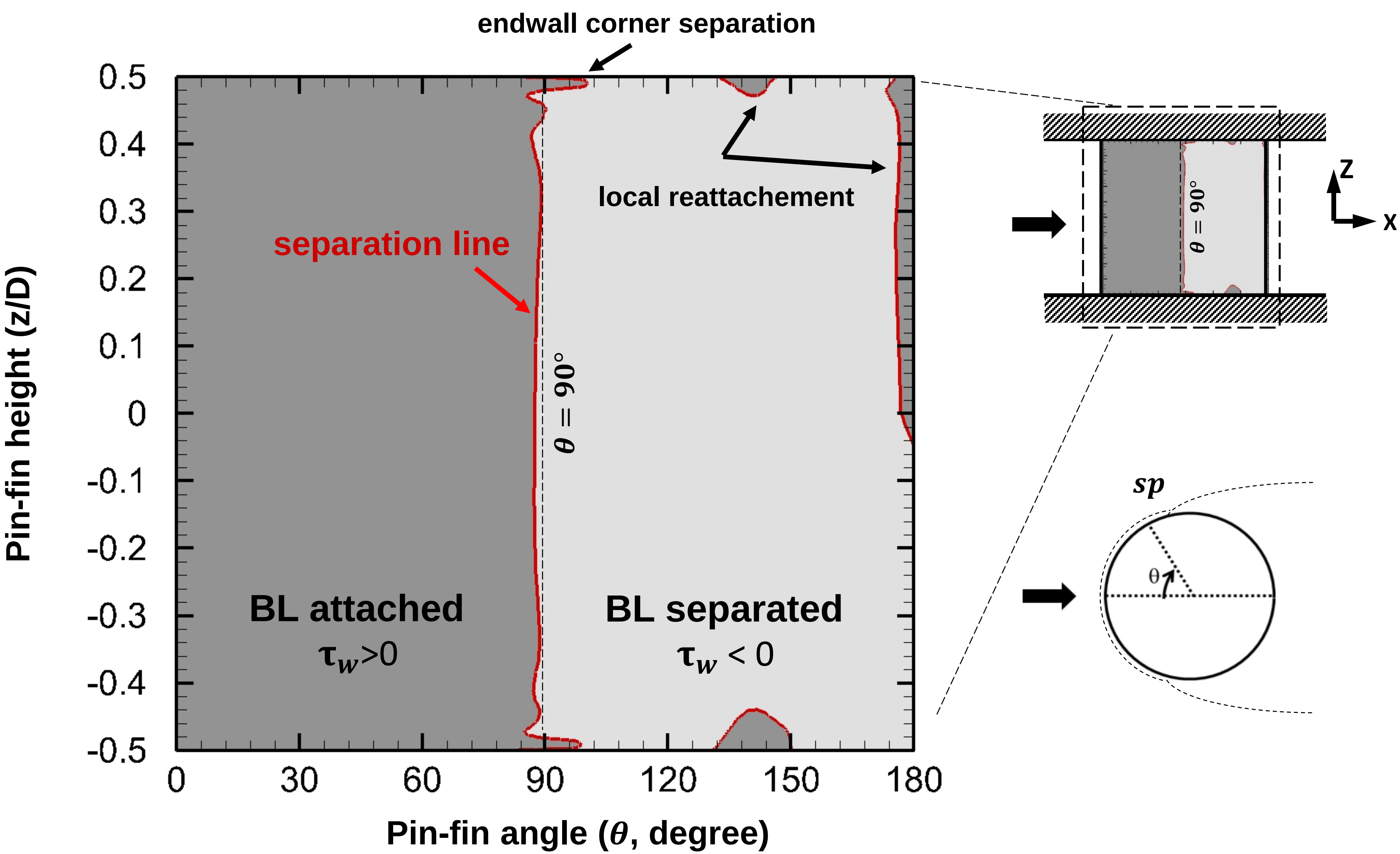

Mean Flow Separation Line

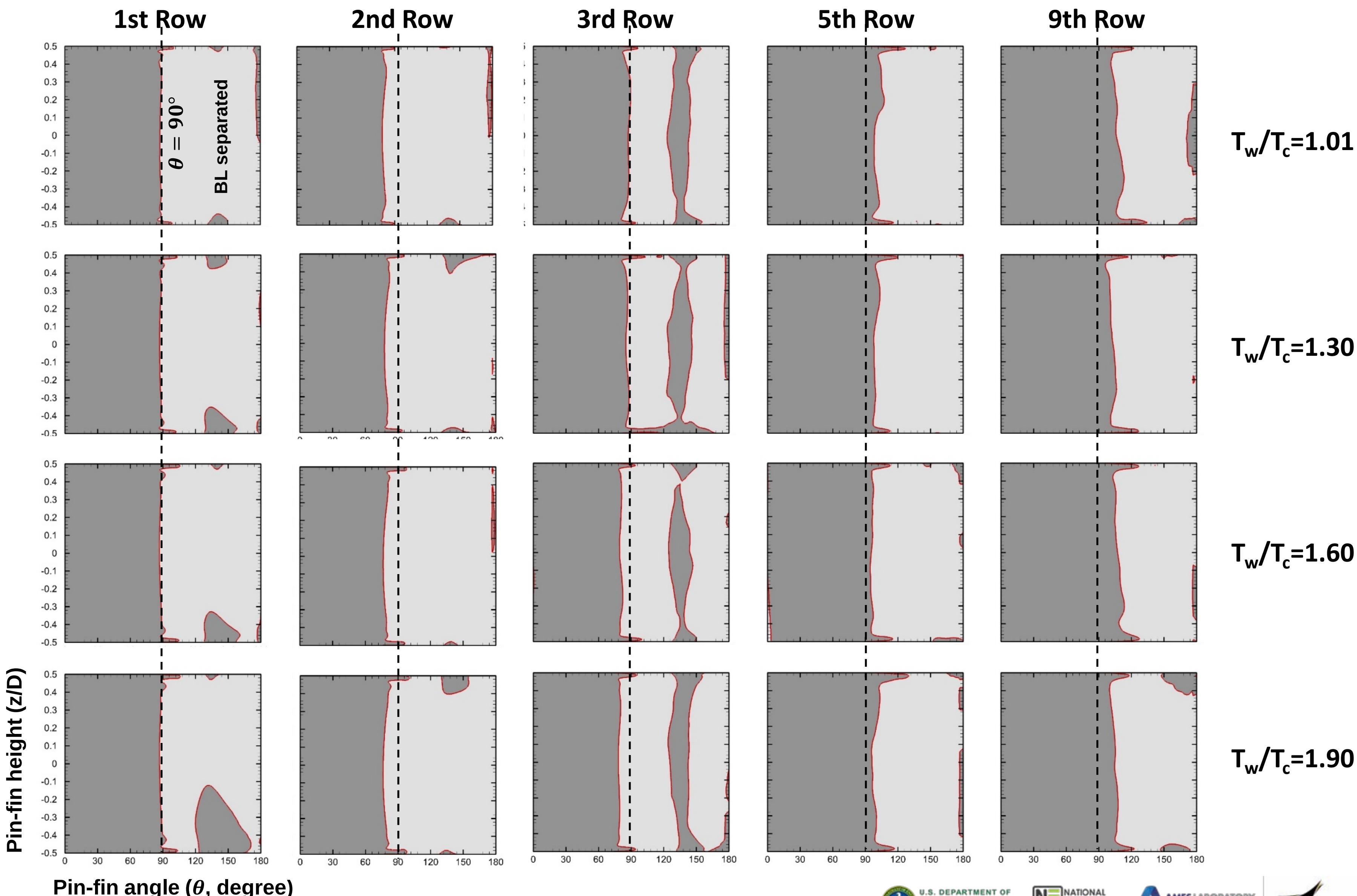

Flow Separation Regime = f(Re)

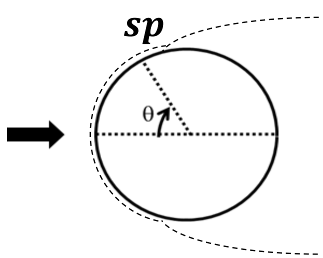

Reynolds number regime	Flow regime	Flow form	Flow characteristic	Strouhal number Sr	Drag coefficient c_D	Separation angle Θ_S
$\frac{150}{300} < \mathrm{Re} < \frac{10^5}{1.3 \cdot 10^5}$	Subcritical regime		Laminar, with vortex street instabilities	Sr = 0.21	$c_D \approx 1.2$	$\Theta_S \approx 80°$
$\frac{10^5}{1.3 \cdot 10^5} < \mathrm{Re} < 3.5 \cdot 10^6$	Critical regime	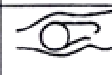	Laminar separation Turbulent reattachment Turbulent separation Turbulent wake	No preferred frequency	$0.2 < c_D < 1.2$	$80° < \Theta_S < 140°$
$3.5 \cdot 10^6 < \mathrm{Re}$	Supercritical regime (transcritical)		Turbulent separation	$0.25 < \mathrm{Sr} < 0.30$	$c_D \approx 0.6$	$\Theta_S \approx 115°$

Ref: H. Schlichting

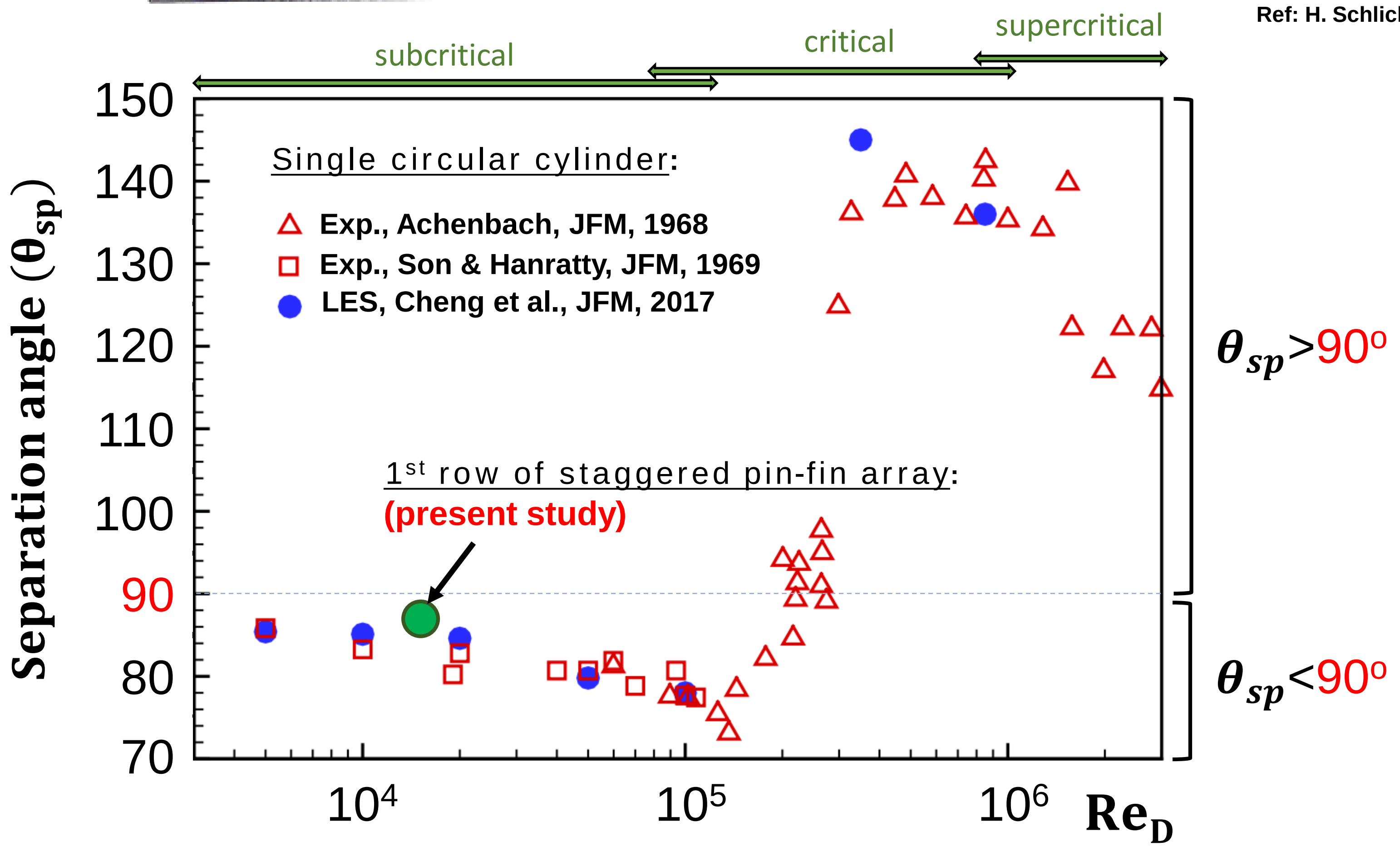

Pressure Coefficient on Pin-Fins

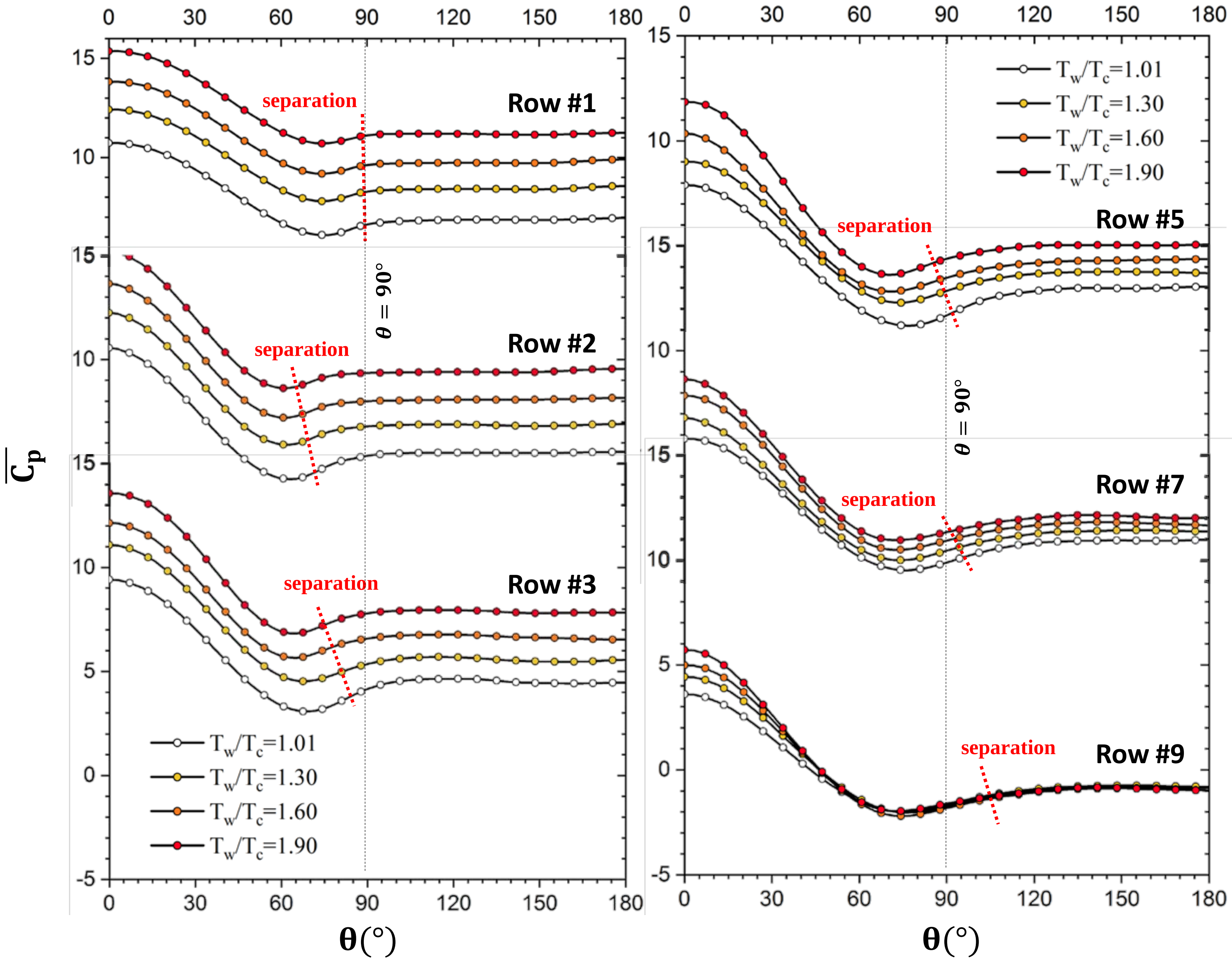

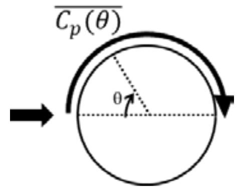

$$\overline{C_p(\theta)} = \frac{\overline{P(\theta)} - P_b}{0.5\rho V_c^2}$$

- As the heat load increases, adverse pressures on the pins become stronger, causing the occurrence of separation earlier.
- The pressure drag in the entrance region would be affected significantly by higher heat loads.

Wall Shear Stress on Pin-Fins (Center Plane)

- The wall shear stress on the pin-fin surface becomes stronger as the heat load increases, which would arise the associated viscous drag in the pin-fin array significantly.
- As the heating load increases, the corresponding wake separation occurs earlier.

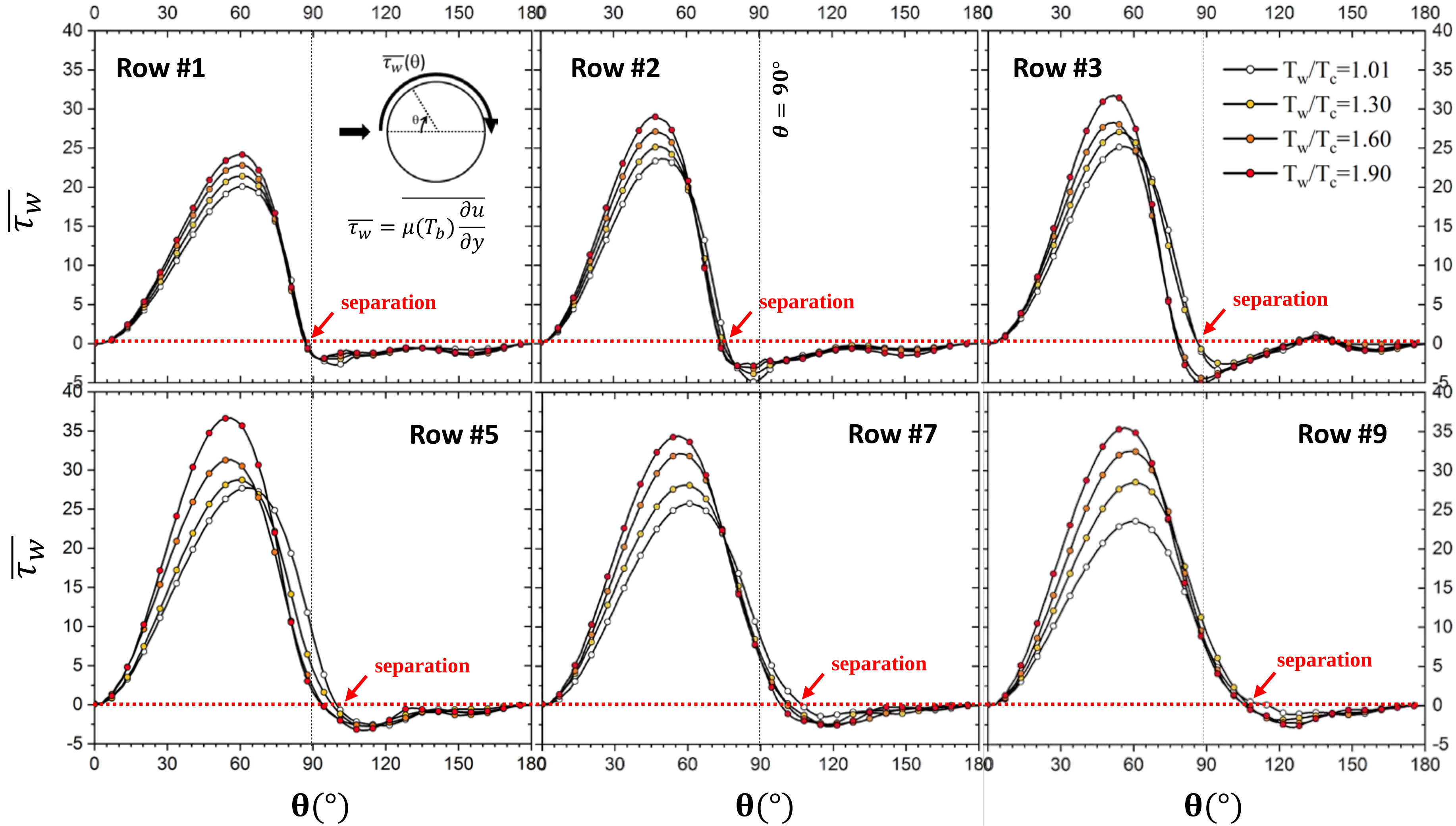

Flow Separation Angle (center plane)

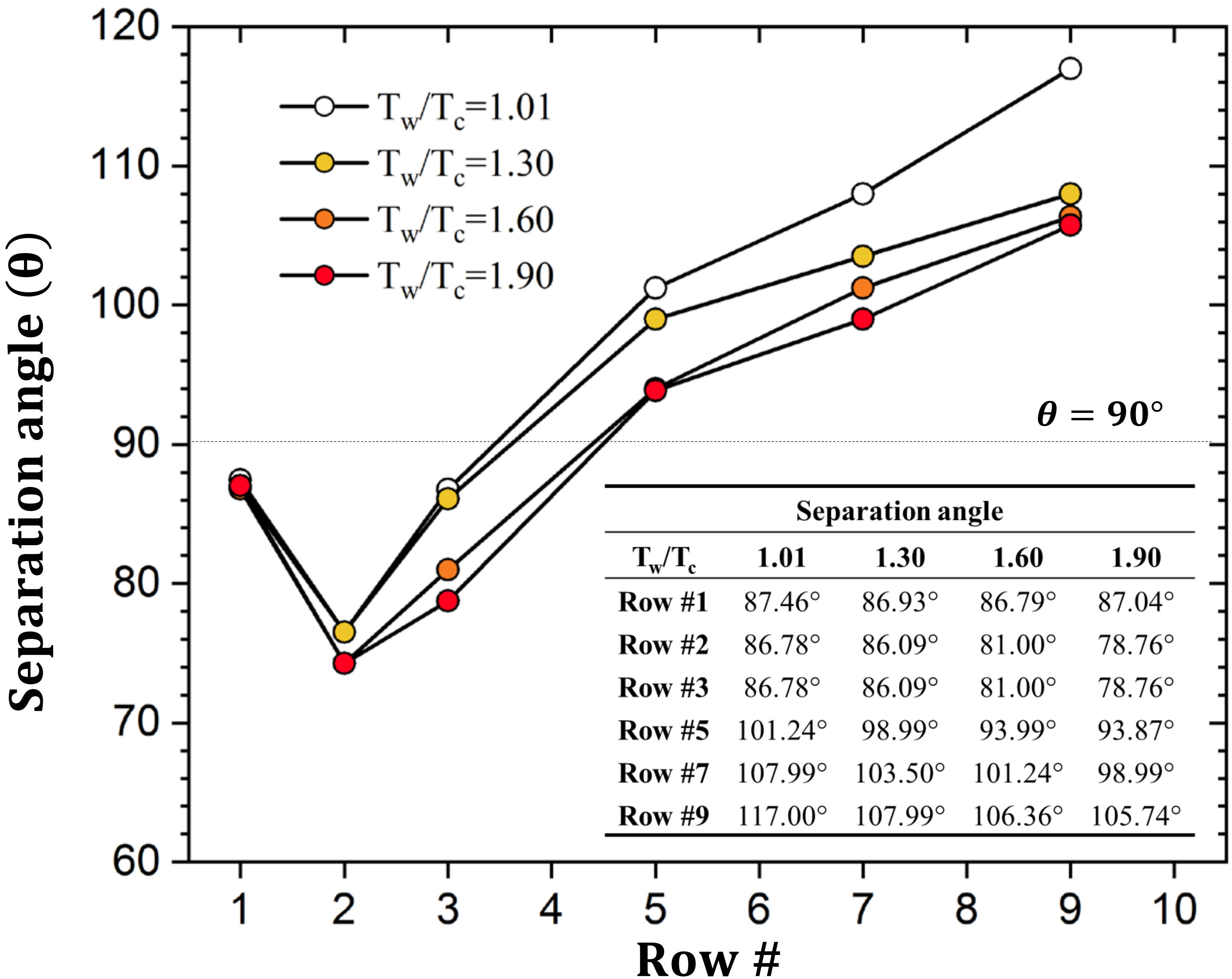

Separation angle				
T_w/T_c	**1.01**	**1.30**	**1.60**	**1.90**
Row #1	87.46°	86.93°	86.79°	87.04°
Row #2	86.78°	86.09°	81.00°	78.76°
Row #3	86.78°	86.09°	81.00°	78.76°
Row #5	101.24°	98.99°	93.99°	93.87°
Row #7	107.99°	103.50°	101.24°	98.99°
Row #9	117.00°	107.99°	106.36°	105.74°

Vortex Shedding Mechanism

Instantaneous Vortex Shedding

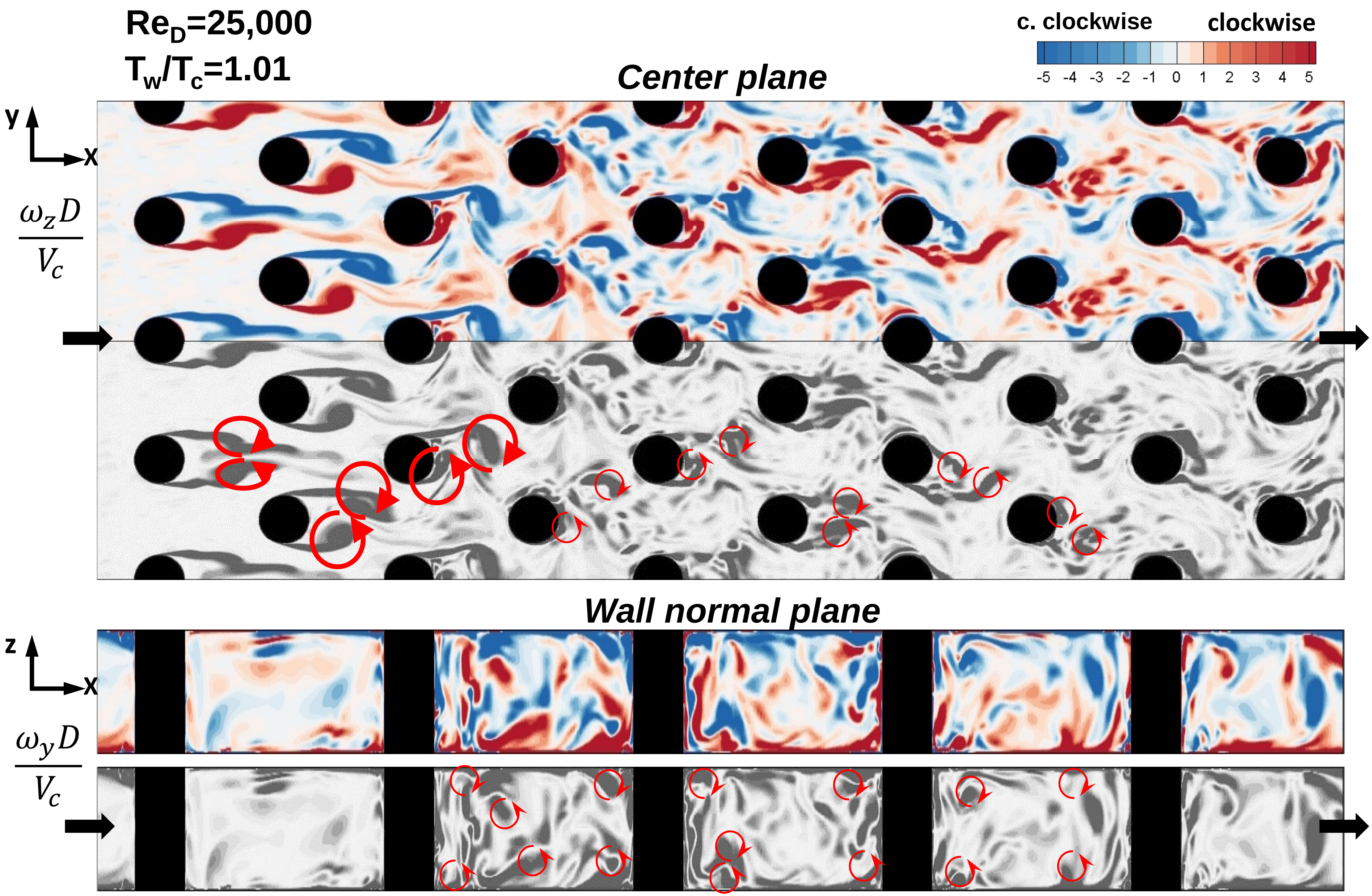

Evolution of Wake Shedding

(Center Plane, Colored by $\omega_z D/U_{ref}$)

LOW **Heat load (T_w/T_c=1.01)** HIGH **Heat load (T_w/T_c=1.90)**

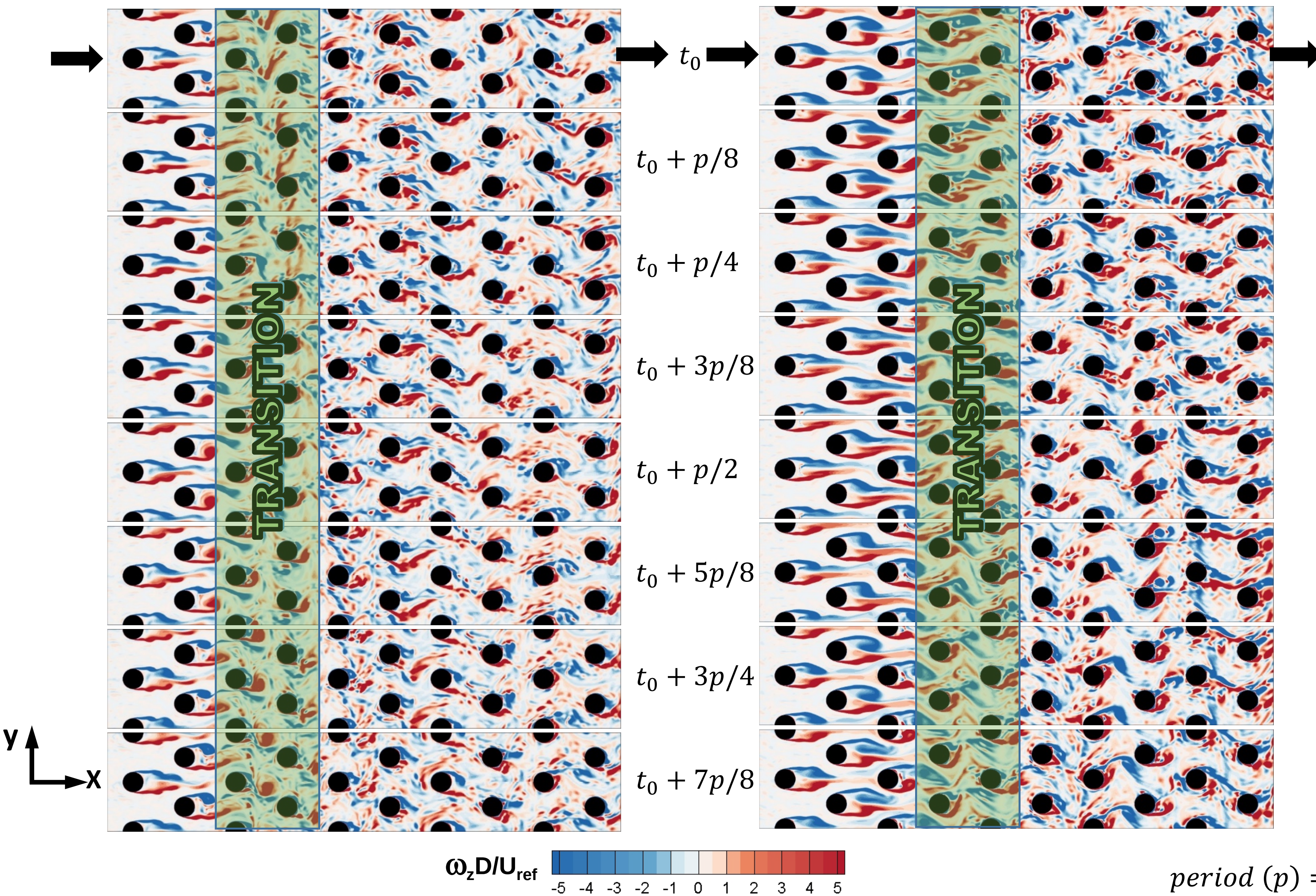

$period\ (p) = 2ms$

Mean & RMS Streamwise Velocity Profiles

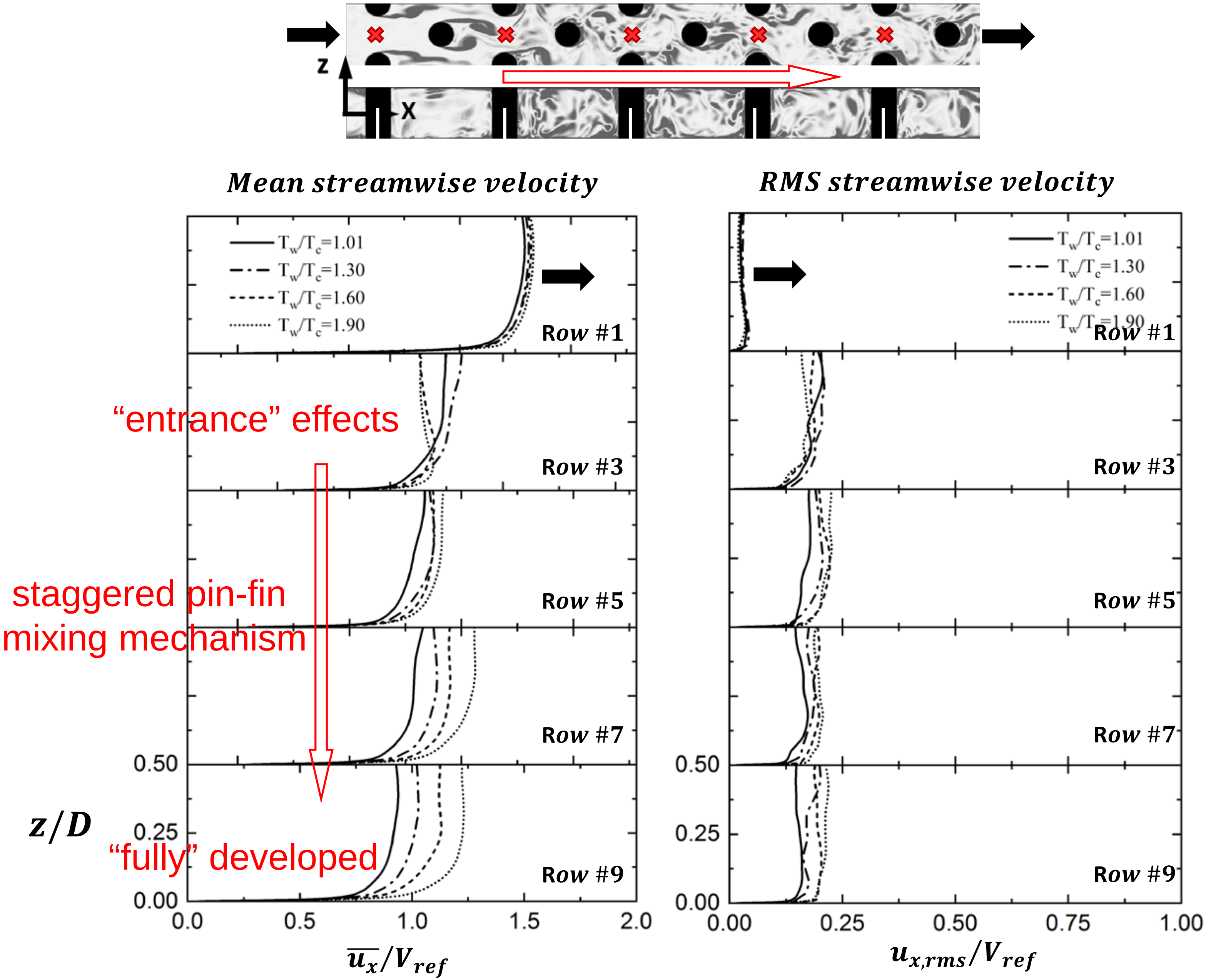

Evolution of Wake Shedding

(Wall Normal Plane, Colored by $\omega_y D/U_{ref}$)

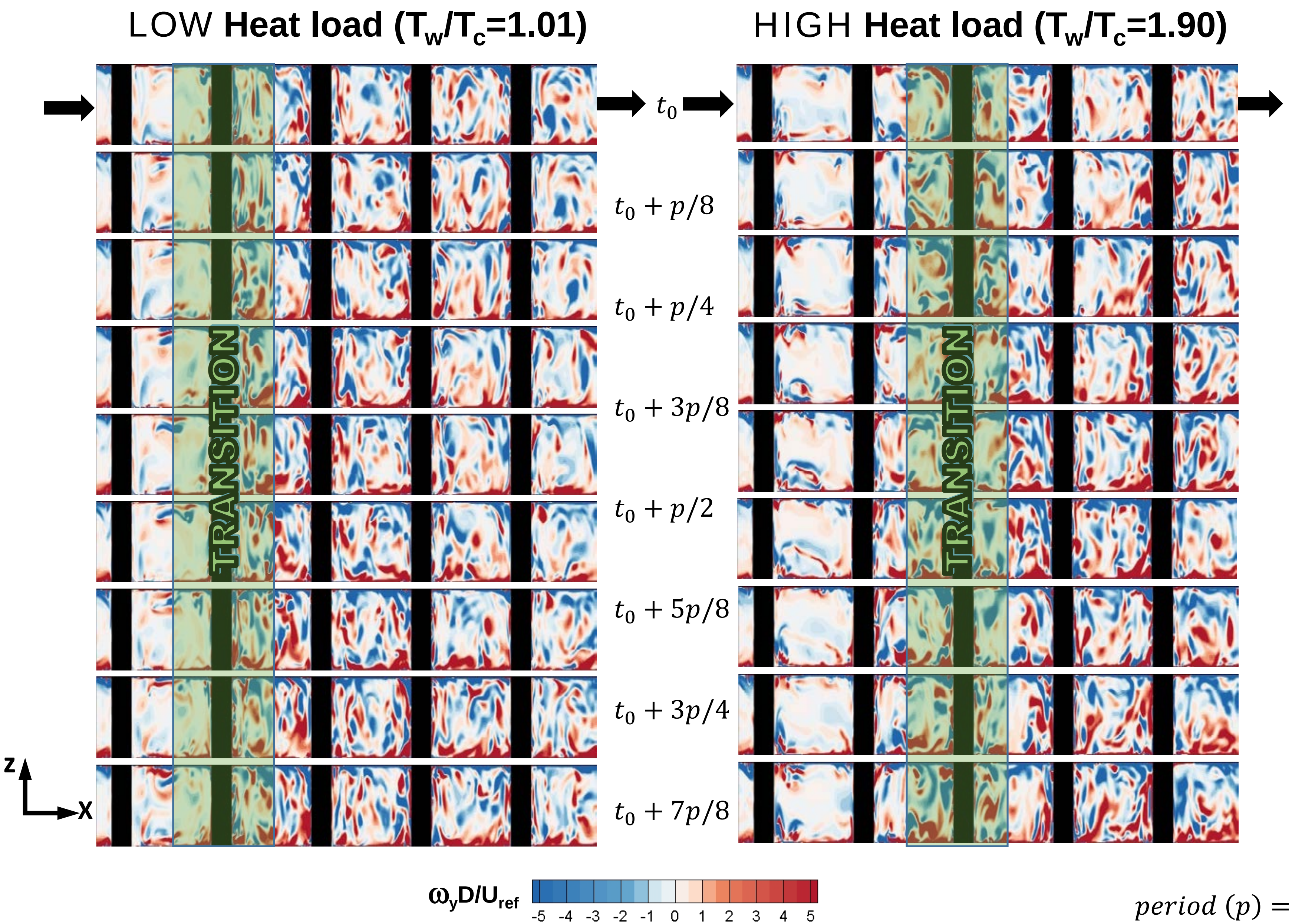

$period\ (p) = 2ms$

Wake Shedding Amplitude & Frequency

- The shedding amplitude increases over the rows in the streamwise direction.
- The wake shedding frequency due to the vortex shedding instability varies from 368Hz- 553 Hz with corresponding amplitude of unsteady flow fluctuation in the order of 1-3 m/s.

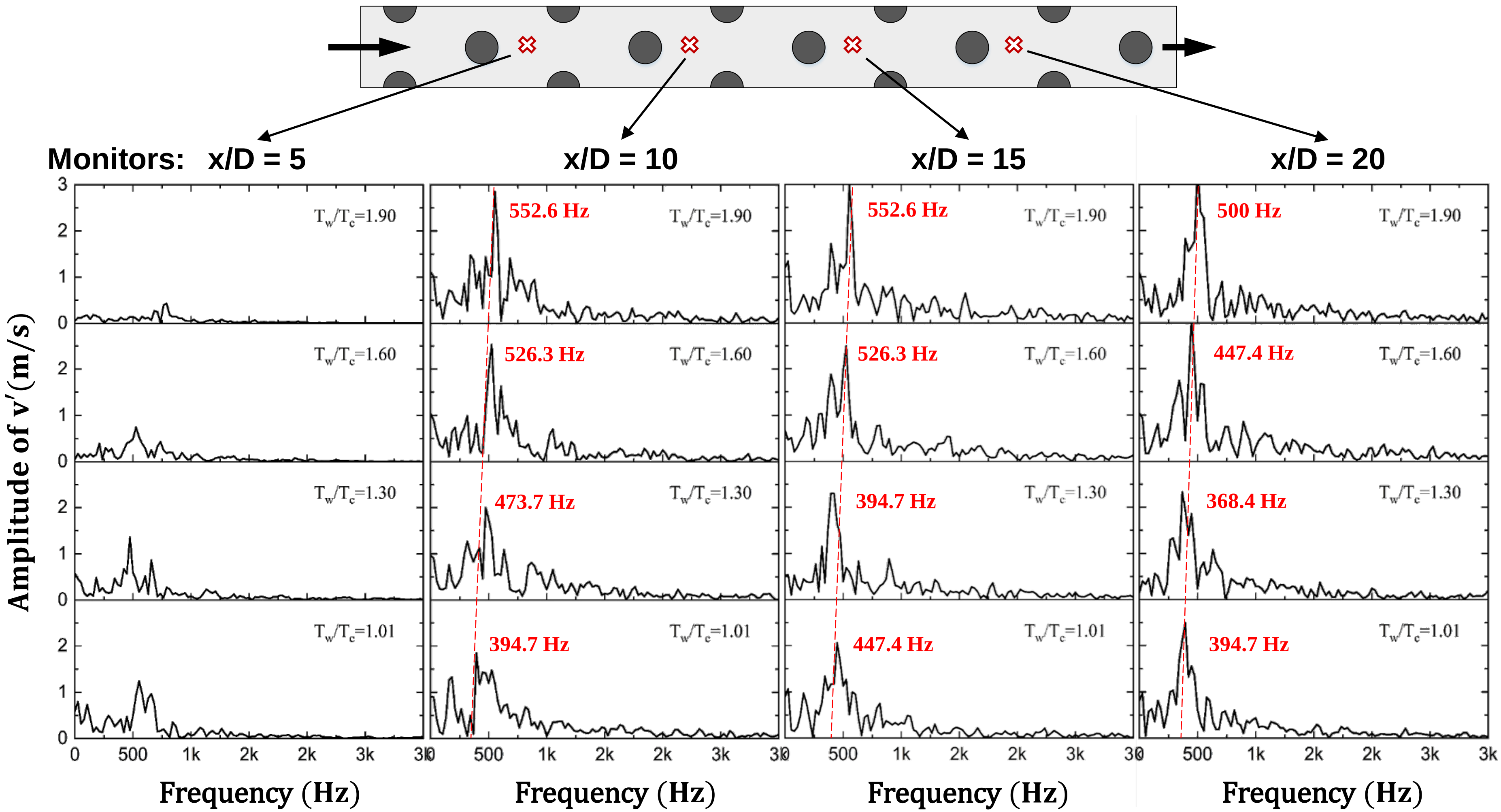

Wake Shedding Energy Spectrum: E_{vv}=f(frequency)

- Performed FFT to the monitored spanwise velocity component to compute the energy spectrum as a function of time signals
- The peak of frequency increases as heat loads increase.
- **Very small scales can be detected by SAS (largest resolved frequency = 5 x 10^4 Hz)**

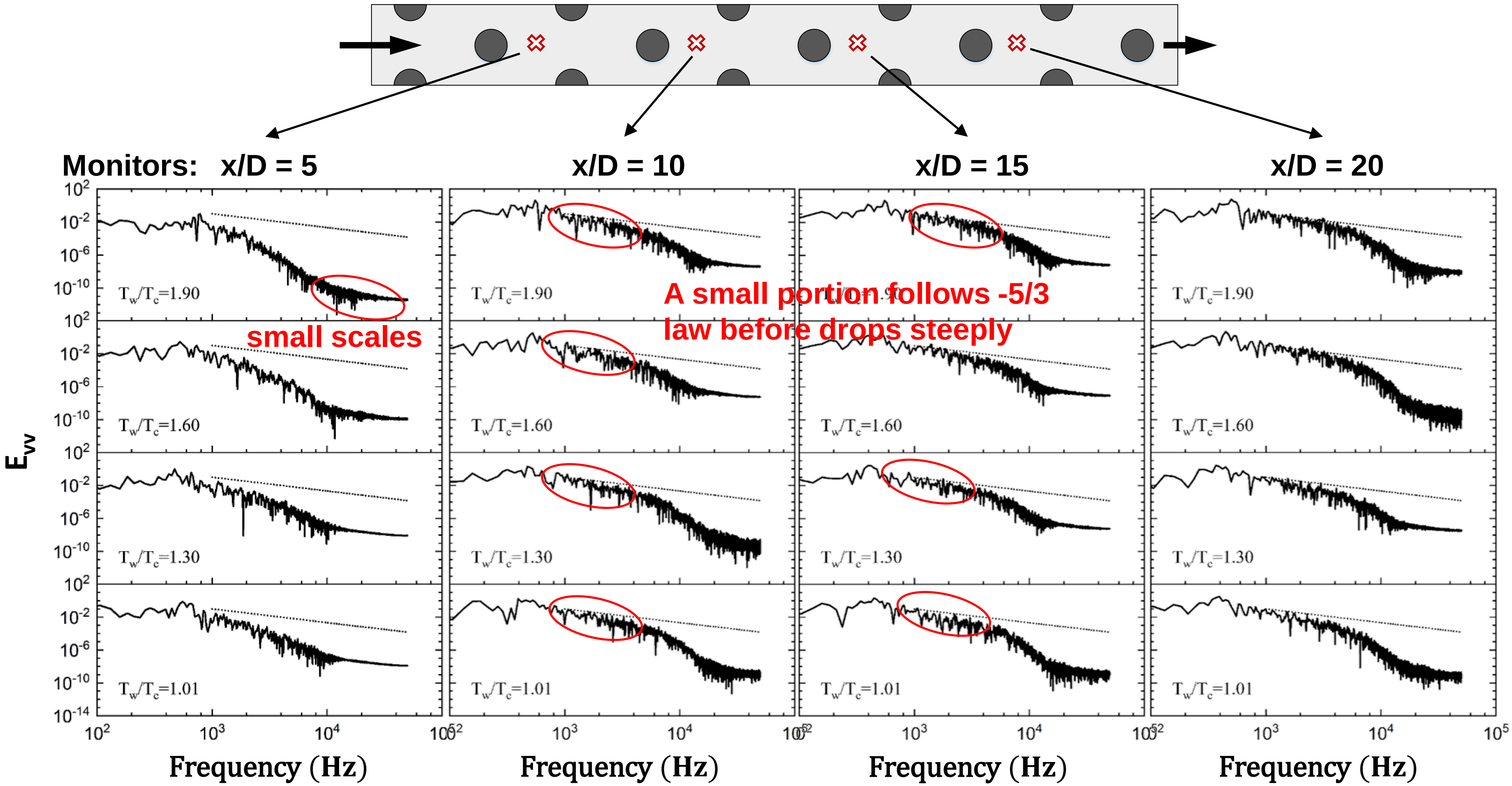

Characteristic Frequency (Strouhal number, St)

- Two spectral peaks can be identified as St_1 and St_2 in the regime of Re=25K, H/D=1, $S_x/D=S_y/D=2.5$
- St_1 is not affected by the heat loads.
- St_2 signal varies with the heat loads over rows

		H/D	Re_D	St
Single circular cylinder		-	20,000	0.21
	Ames & Dvorak, 2006	2	10,000/30,000	0.234/0.209
Pin-fin array (1st Row)	Ostanek & Thole, 2012	2	20,000	0.18
	Present study	**1**	**25,000**	**0.248**

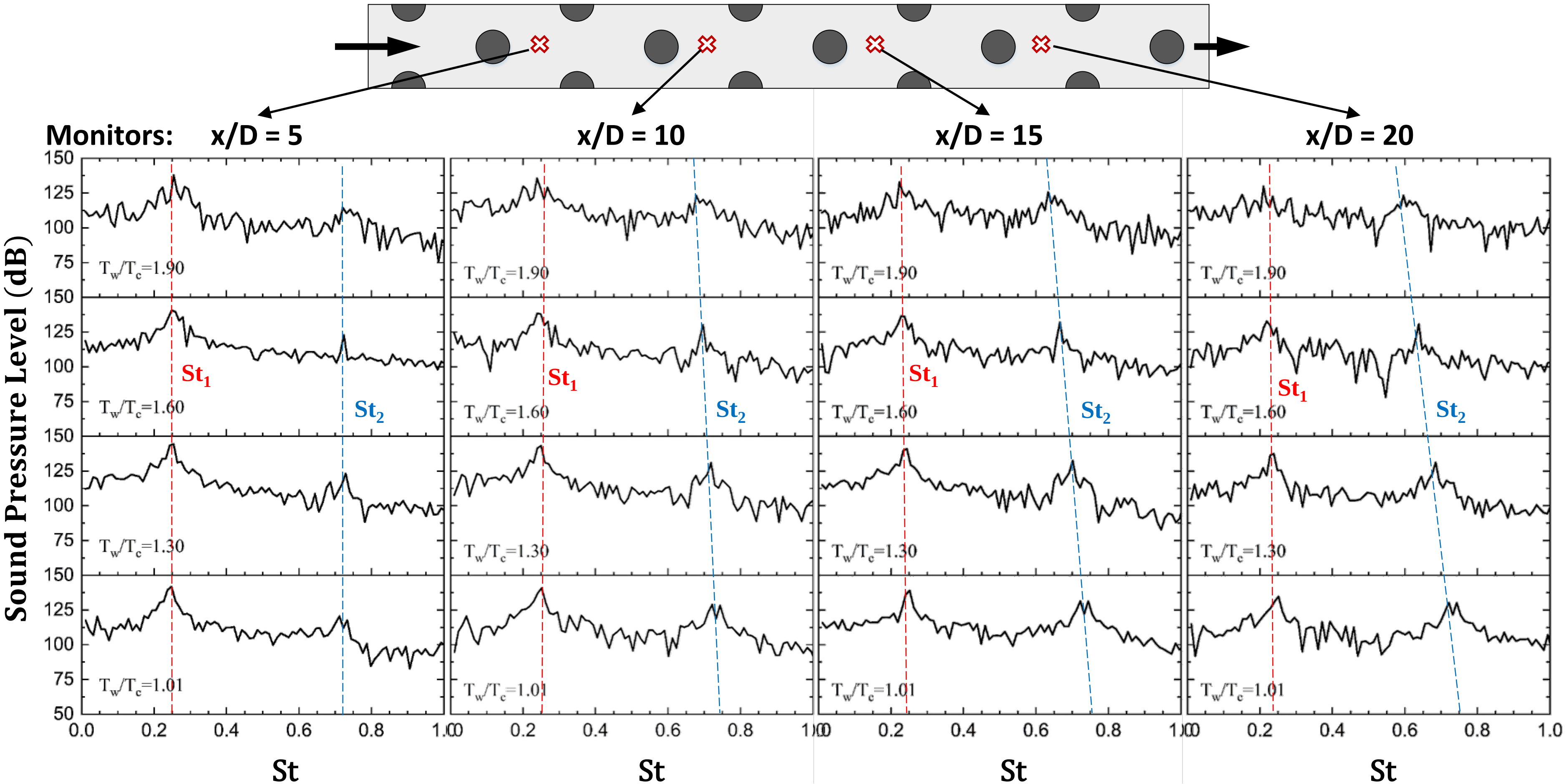

Correlation for Nu=f(Re, Pr, T_w/T_b) Lab & Engine Conditions

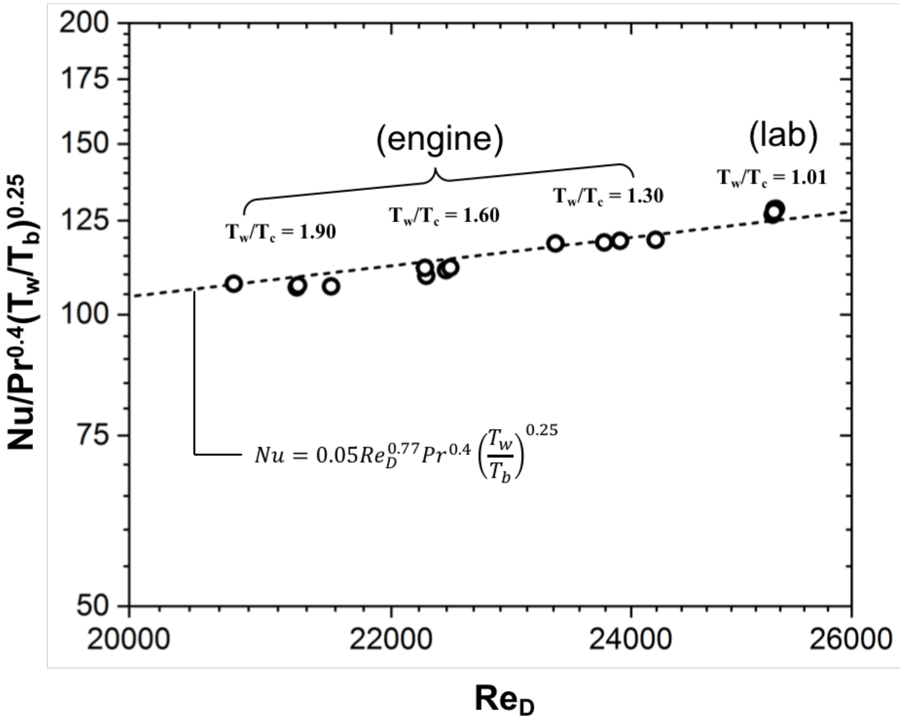

Heat load (T_w/T_c)	1.01	1.30	1.60	1.90
T_w/T_b	1.005	1.161	1.293	1.399
Re_D	25,279	23,350	22,270	20,776

For HX w/ short pin-fins under lab and engine-relevant conditions:

- H/D=1, $S_x/D=S_y/D=2.5$
- Re_D: 20,000-25,000
- Pr: 0.69-0.72
- T_w/T_c: 1.01-1.90

A correlation equation of Nu=f(Re, Pr, T_w/T_b) in the fully developed region is found:

$$Nu=0.05Re_D^{0.77}Pr^{0.4}(T_w/T_b)^{0.25}$$

Summary

- High heat loads cause considerable transport property changes over the rows:
  - The mean bulk temperature arises 22%.
  - The mean Reynolds number drops up to 20%.
  - The mean Prantdl number increases up to 4%.
- High heat loads along the duct were found to affect the locations where unsteady flow separation take place about pin fins, the magnitude of the vorticity shed in the wakes, and the shedding Strouhal number. These unsteady flow mechanisms in turn strongly affect the nature of the surface heat transfer.
- As the heat load increases, the surface heat transfer decreases. Nu increases over the front rows in the entrance region and reaches to its maximum at the 4th row. Nu appears to be not strongly affected by the heating loads at the 5th row, where there occurs a transition from the entrance region (Rows 1-4) to the so-called fully developed region (Rows 6-10).
- Still working on understanding the flow and its effects on heat transfer and why RANS is unable to predict correctly the HTC in the 2nd and 3rd rows.

Thank you! Questions? Comments?

My thanks to my students at Purdue who do all the work.

U.S. DEPARTMENT OF ENERGY

NATIONAL ENERGY TECHNOLOGY LABORATORY

AMES LABORATORY
Creating Materials & Energy Solutions
U.S. DEPARTMENT OF ENERGY

PURDUE AERONAUTICS & ASTRONAUTICS